13th Australasian Fluid Mechanics Conference
Monash University, Melbourne, Australia
13-18 December 1998

WALL SHEAR STRESS IN CLEARANCE GAP OF BLOOD PUMP MODEL

CHUA L. P., WONG S. S., TUNG S. C. and CHAN W. K.

School of Mechanical and Production Engineering
Nanyang Technological University, Nanyang Avenue, Singapore 639798, SINGAPORE

ABSTRACT

This paper presents the measurements of fluid wall shear stress in the clearance gap between the impeller face and inlet casing of a 5:1 blood pump model. Investigation was made using hot-wire and cold-wire anemometries, as well as a rotating-disk apparatus for calibration. It was found that shear stress values at the eye and peripheral, as well as the middle, of the impeller are critical as these are the regions of high and low stresses respectively.

INTRODUCTION

A magnetically-suspended centrifugal blood pump which eliminates the use of a mechanical drive shaft, seals and bearings has demonstrated its superiority as an artificial heart (Tsukiya et al, 1997). However, animal trials revealed significant hemolysis and thrombosis prevalent in the 0.2mm clearance gaps between the impeller shroud surfaces and pump casing (Akamatsu et al, 1995).

One technique to reduce hemolysis and thrombosis is improvement of the pump design, of which the size of the clearance gap is an important parameter. Gaps that are too small would not allow sufficient washout of blood cells thus leading to thrombus formation while large gaps might give rise to vortex development causing hemolysis. To optimize the design of the blood pump, it is therefore necessary to understand the flow in the clearance gaps.

It has been known that wall shear stress has significant implications on the performance of a blood pump. Too low a value suggests thrombi formation whereas excessive levels can cause hemolysis, the precise threshold value depending on shear exposure time and surface of contact (Brown et al, 1975, Sallem and Huang, 1984). For this purpose, wall shear stress measurements were conducted on the fluid flow in the front clearance gap of a pump model scaled up five times according to specifications so that studies can be easier done on the magnified clearance gap (Chua et al, 1998a).

EXPERIMENTAL METHOD

The pump model in Figure 1 was enlarged from the prototype design based on dimensional analysis (Chua et al, 1998a). The wall shear stress was obtained using hot-wire and cold-wire anemometers, and a rotating disk apparatus. The probe, see Figure 2, consists of a hot wire (ϕ5μm Wollaston Pt 10%-Rh), operated under constant temperature anemometer (CTA), and a cold wire (ϕ1.2μm Wollaston Pt 10%-Rh), operated under constant current anemometer, soldered onto brass prongs inserted through

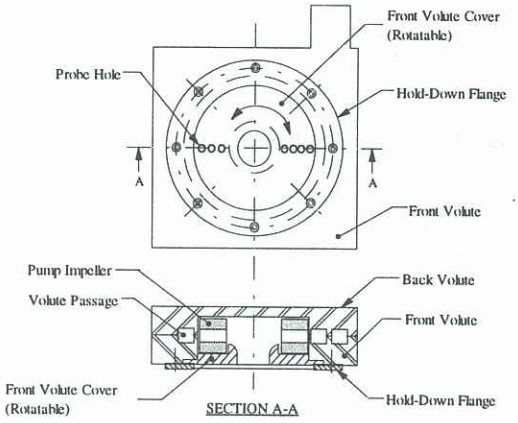

Figure 1 : Schematic of pump model

the probe measuring surface. The wires were laid parallel to each other and flat on the probe before the silver coating was etched away exposing ≈1mm of the wires.

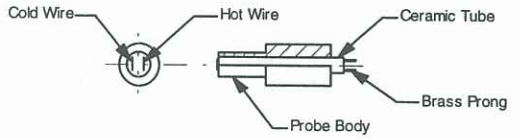

Figure 2 : Wall shear stress probe

A rotating disk apparatus as shown in Figure 3 was used as a calibration rig for the wall shear stress probe. Briefly, the calibration rig consists of a stationary disk, a rotating disk and a motor. The probe could be placed in the stationary disk at a fixed radial location and the gap between the stationary and the rotating disks were maintain at a constant value. The rotating disk was coupled directly to a motor which was mounted under a table. To obtain a consistently parallel gap between the rotating and stationary disks, three micrometer heads were fixed onto stands extending from the table top to tune the clearance gap between the two disks. The micrometer head non-rotating spindles were then tightened onto the stationary disk at 120° apart. A detailed description of the calibration rig can be found in Chua et al (1998b).

For calibration, the probe was mounted flush at a fixed radial position on the stationary plate while the rotating disk span at a distance away facing the probe. The wall

shear stress τ_w can be expressed as (Brown and Davey, 1971)

$$\tau_w = \mu\left(\frac{r\omega}{d}\right)\left(1+\frac{Re^2}{1050}+\ldots\right) \qquad \ldots\ldots\ldots(1)$$

where μ is the kinematic viscosity, r the probe radial position, ω the disk rotational speed, d the calibration

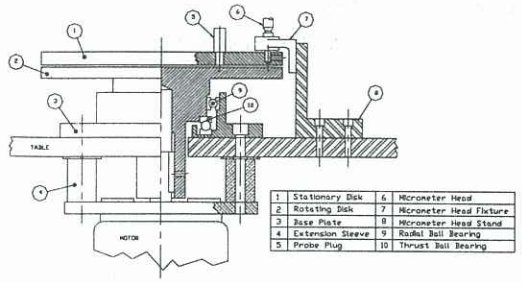

Figure 3 : Probe calibration rig set-up

gap and *Re* the fluid Reynolds number. By varying any of the three parameters (r, ω and d) in Eq. (1), the relationship (calibration constants A and B) between the wall shear stress and probe output voltage E can be determined by (Geremia, 1972)

$$E^2 = A + B\tau_w^{1/3} \qquad \ldots\ldots\ldots(2)$$

It was found later that the linear relationship between E and τ_w in Eq. (2) is not well presented for low wall shear stress measurements, and a parabolic relation is used as shown in Eq. (3)

$$E^2 = A + B\tau_w^{1/3} + C\tau_w^{2/3} \qquad \ldots\ldots\ldots(3)$$

The difference in temperature between calibration and measurement due to air viscosity must be accounted for through (Perry, 1982)

$$E_c = E + \left.\frac{\partial E}{\partial T}\right|_{\tau_w}(\Delta T) \qquad \ldots\ldots\ldots(4)$$

in which E_c and E are the compensated and measured CTA voltages respectively, $\left.\frac{\partial E}{\partial T}\right|_{\tau_w}$ the change in CTA voltage with respect to temperature at constant τ_w. The temperature difference between the reference (ambient) and measurement point ΔT is given by

$$\Delta T = \frac{GIR\alpha}{\Delta V} \qquad \ldots\ldots\ldots(5)$$

such that G, I and ΔV are correspondingly the CCA gain, current and voltage change whereas R and α are cold-wire resistance and temperature coefficient of resistivity.

Prior to every set of measurement, the temperature derivative in Eq. (4) i.e. $\left.\frac{\partial E}{\partial T}\right|_{\tau_w}$ will firstly be determined. The hot-wire and cold-wire probe was first put in a certain radial position of the calibration rig. The reference (ambient) temperature of the probe was taken by placing a portable K-type thermometer between the rotating and stationary plates. By keeping the motor speed, radial position of the probe and the gap between the disks constant, the output of the CTA and CCA were taken at 5 minutes' interval. After about seven sets of readings, the temperature derivative in Eq. (4) could be determined. The calibration constants for the hot-wire in Eq. (3) would then determined by varying the speed of the motor but keeping r and d constant. A sample of 999 voltages each from the CTA and CCA were digitized by a 12-bit analog-to-digital converter before input into a computer for processing. Both the temperature derivative and the calibration constants were obtained by least squares method, and fed into the second part of a computer program which converted the hot-wire voltages into wall shear stresses; the mean value was then determined from the 999 samples. To reduce the effect of wire drift, the duration between successive calibrations was kept within 1 hour.

For measurement of the wall shear stress, seven holes were drilled across the diameter of the front volute cover of the pump at radius (in mm) r=69.5, 78, 86.5, 95, 103, 112 and 120 as shown in Figure 1. Only one wall shear stress probe was used in a particular radial position at a time. This is to prevent the interruptions on the internal surface of the pump volute, creating eddies at the protrusions made by the probes. Note that the other six holes are flushed with the perspex cover during measurement. After the wall shear stress probe has been calibrated in the calibration rig, the probe was transferred and inserted into the front volute cover of the pump. At the beginning of measurement the front volute was rotated to the 0° position. After tightening the volute and ensuring that there was no obstruction in the pump, the motor was started with its speed set at a constant rate. For the present preliminary measurement, the inlet was fully opened with three different flow coefficients of $\Phi = Q/(2\pi rb\omega^2) = 0.078$, 0.04 and 0. Note that Q is the flow rate and b is the thickness of the pump impeller blade. The wall shear stress measurements were obtained at an angular interval of 5°. Estimates of the random component of uncertainty for mean and rms wall shear stresses were ±2.8% and ±1.7% respectively.

RESULTS AND DISCUSSION

Figures 4(a) and (b) show the Cartesian and polar plots of the wall shear stress distributions at various radial positions for $\Phi = 0.078$ respectively. It can be observed in Figure 4(a) that for $\Phi = 0.078$ the stress values for 120.5mm, 112mm and 69.5mm radii are high. The trends for the two outer most radii (120.5mm and 112mm) are similar, though the former shows higher stress values. There are two peaks at 50° and 195° angular positions, and a mound at 345°. Occurrences of the two peaks are after the 'tongues' of the double-spiral volute (see schematic at the side of Figure 4(b)). Note that the

double-volute design was adopted to balance radial thrust acting on the magnetically-suspended impeller as well as minimize the electrical power required to levitate it. The rise in the stress value in the 'tongue' regions could be due to the change in geometry of the casing, which may have caused the flow to be more turbulent. Stress values for 69.5mm radius exhibit less variation, maintaining at a high level until 235° where they decrease, but slowly increase to a spike at 330°. This pattern may be influenced by the air intake at the eye of the impeller, which cause the high stress values.

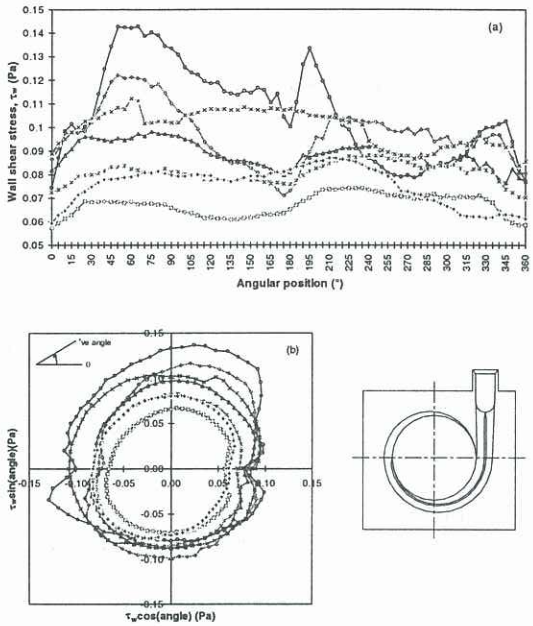

Figure 4 : Wall shear stress for $\Phi = 0.078$ in (a) Cartesian plot and (b) Polar plot (Refer to Figure 5 for caption)

The wall shear stresses at 103.5mm, 95mm, 86.5mm and 78mm radii show a similar trend. These four sets of stresses do not fluctuate as much as 120.5mm and 112mm radii. The wall shear stress values are generally low for these four radii. Out of the four radii, 103.5mm shows the highest stress values, followed by 86.5mm and then 78mm. 95mm radius gives the lowest stress values.

The wall shear stress values for $\Phi = 0.0$ at the different radii show a 'W' shape in Figure 5(a). Two peaks can be seen at 0° and 180° angular positions, and the graph is symmetrical at 180° (see Figure 5(b)). The wall shear stress values are high at the 'tongues' of the double-spiral volute and low at the other angles.

It can be seen that 120.5mm radius gives the highest stress value at 0° angular position. The stress decreases with decreasing radius, i.e. towards the impeller eye. That is to say, 120.5mm radius gives the highest stress values and 69.5mm radius the lowest. This does not correspond to the stress values taken for the fully opened condition (i.e. $\Phi = 0.078$), as for the fully closed condition (i.e. $\Phi = 0.0$), no air is taken into the pump through the eye of the impeller, so air only circulates in it. Thus the stress values are low at these regions.

Stress values are high at the 'tongues' of the volute (0° and 180° angular positions). This could be due to the change in volute geometry. However, in the actual case, the blood pump will not operate under this fully closed (zero flow rate) condition, except during surgery when the flow rate may be stopped for a few seconds. Nonetheless, it is very unlikely that this condition will be encountered in real life. The reason why it was being carried out in this project was to investigate the extreme condition to which the pump can be subjected.

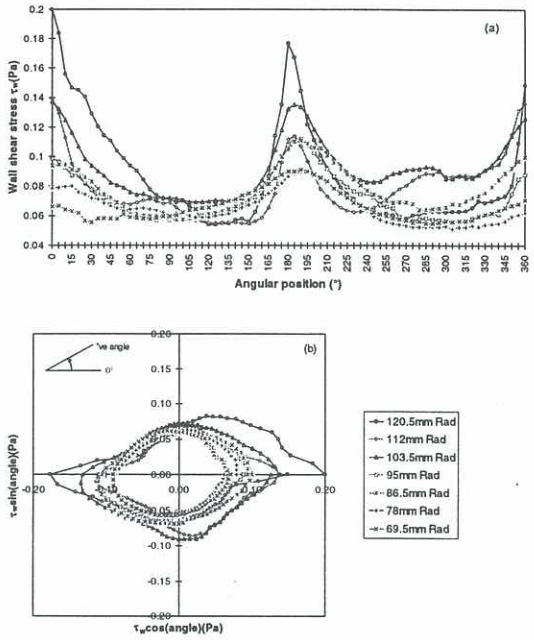

Figure 5 : Wall shear stress for $\Phi = 0.0$ in (a) Cartesian plot and (b) Polar plot

Figure 6(a) shows the wall shear stress at $\Phi = 0.04$ which is about the condition in between the fully open and closed conditions. The figure does demonstrate the characteristics of both the fully opened and fully closed conditions. It can be seen that there are two peaks. The first does not occur at 0° (note that 0° and 360° angular positions are the same point), as in the fully closed condition, but at 10°. However the next peak which occurs at 180° corresponds to the fully closed condition. The stress values taken in the first quadrant (0° to 90°) show some similarity to the fully opened condition.

It can also be observed that 120.5mm radius gives the highest stress values, and they decrease as the radius decreases. The lowest wall shear stress values are given by the two smallest radii, i.e. 69.5mm and 78mm, which are at the eye of the impeller. This is similar to the fully closed condition. It can be concluded that the half flow rate condition shows more similarity to the fully closed condition than fully opened.

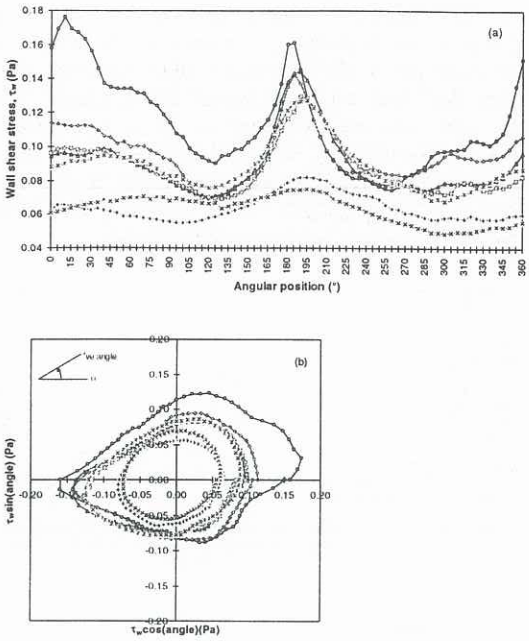

Figure 6 : Wall shear stress for $\Phi = 0.04$ in (a) Cartesian plot and (b) Polar plot (Refer to Figure 5 for caption)

Rms distributions for the wall shear stress are shown in Figures 7(a), (b) and (c) for $\Phi = 0.078$, 0.0 and 0.04 respectively. It can be deduced that radii 120.5mm and 112mm fluctuate the most, which may be due to back-flow of the air at the impeller periphery and 'tongues' of the double-spiral volute. The peak rms values for $\Phi = 0.0$ and 0.04 are much higher than those for the $\Phi = 0.078$ at r=120mm. Moreover, rms values at the eye are surprisingly low which indicates that the flow into the pump is rather smooth resulting in low turbulence level.

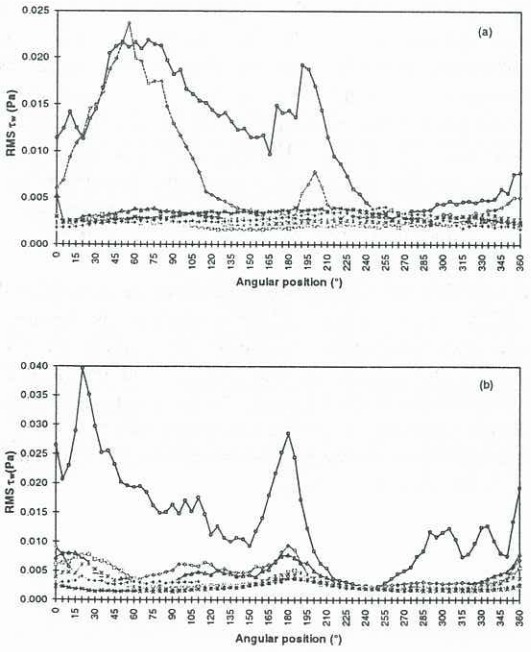

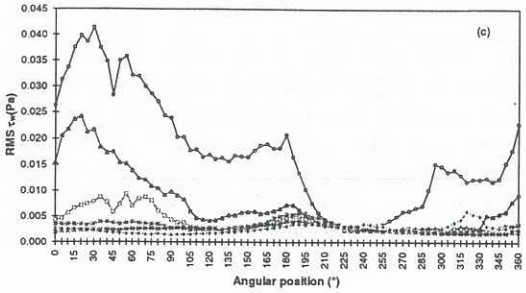

Figure 7 : Rms distributions for (a) $\Phi = 0.078$ (b) $\Phi = 0.0$ and (c) $\Phi = 0.04$ (Refer to Figure 5 for caption)

CONCLUSION

From the measurements of wall shear stress at three different flow conditions, it can be concluded that the wall shear stress values at the eye, peripheral, and middle of the impeller are critical, as these are regions of high and low stresses respectively. Regions of high shear stress are more prone to hemolysis while thrombosis is more likely to take place in regions of low stress. The locations of "tongues" have a great influence on the shear stress distribution; this finding should be useful for future blood pump design.

REFERENCES

AKAMATSU, T., TSUKIYA, T., NISHIMURA, K., PARK, C. H. and NAKAZEKI, T., "Recent studies of the centrifugal blood pump with a magnetically suspended impeller," Artificial Organs, **19(17)**, 631-634,1995.

BROWN, G. L. and DAVEY, R. F., "The calibration of hot films for skin friction measurement," Review of Scientific Instruments, **42(11)**, 1729-1731, 1971.

BROWN, H., LEMUTH, R. F., HELLUMS, J. D., LEVERETT, L. B. and ALFREY, C. P., "Response of human platelets to shear stress," ASAIO Transactions, **21**, 35-39, 1975.

CHUA, L. P., AKAMATSU, T. and CHAN, W. K., "Preliminary measurements of an enlarged blood pump model," Int. Comm. Heat Mass Trans., 1998a (Accepted for publication).

CHUA, L. P., TUNG, S. C. and CHAN, W. K., "Preliminary measurements of wall shear stress," Int. Comm. Heat Mass Trans., 1998b (Accepted for publication).

GEREMIA, J. O., "Experiments on the calibration of flush mounted film sensors," DISA Info., **13**, 5-10, 1972.

PERRY, A. E., "Hot-wire anemometry," Oxford, University Press, New York, 1982.

SALLEM, A. M. and HUANG, N. H. C., "Human red blood cell hemolysis in a turbulent shear floe, contribution of Reynolds shear stress," Biorheology, **21**, 783-797, 1984.

TSUKIYA, T., AKAMATSU, T. and OZALI, T., "Fluid dynamic design of Kyoto-NTN magnetically suspended centrifugal blood pump," Proc. Of ASME Fluids Engg., Div. Summer Meeting, FEDSM **97-3425**, 1, 1997.